CONVERGENCE OF SIMPLE ADAPTIVE GALERKIN SCHEMES BASED ON H-H/2 ERROR ESTIMATORS

S. FERRAZ-LEITE, C. ORTNER, AND D. PRAETORIUS

ABSTRACT. We discuss several adaptive mesh-refinement strategies based on h-$h/2$-error estimation. This class of adaptive methods is particularly popular in practise since it is problem independent and requires virtually no implementational overhead. We prove that, under the saturation assumption, these adaptive algorithms are convergent. Our framework applies not only to finite element methods, but also yields a first convergence proof for adaptive boundary element schemes. For a finite element model problem, we extend the proposed adaptive scheme and prove convergence even if the saturation assumption fails to hold in general.

1. INTRODUCTION

Let $\mathcal{H}$ be a real Hilbert space with scalar product $\langle\!\langle \cdot\,,\,\cdot \rangle\!\rangle$ and associated energy norm $|||\cdot|||$. Given a right-hand side $F \in \mathcal{H}^*$, we aim at a numerical approximation of the unique solution $u \in \mathcal{H}$ of

$$\langle\!\langle u\,,\,v\rangle\!\rangle = F(v) \quad \text{for all } v \in \mathcal{H}. \tag{1}$$

To that end, let X_ℓ be a finite-dimensional subspace of $\mathcal{H}$, which in many applications is based on a triangulation $\mathcal{T}_\ell$ of some physical domain. Let $u_\ell \in X_\ell$ be the corresponding Galerkin solution, obtained by solving the finite-dimensional linear system

$$\langle\!\langle u_\ell\,,\,v_\ell\rangle\!\rangle = F(v_\ell) \quad \text{for all } v_\ell \in X_\ell. \tag{2}$$

Throughout, the index $\ell \in \mathbb{N}_0 := \{0, 1, 2, \dots\}$ denotes the step of an adaptive algorithm, and associated quantities are discrete and numerically computable.

The h-$h/2$-error estimation strategy is a well-known technique for the a posteriori estimation of the error in the energy norm $|||u - u_\ell|||$: Let $\widehat{\mathcal{T}}_\ell$ be a uniform refinement of $\mathcal{T}_\ell$ and let $\widehat{X}_\ell$ be the associated finite-dimensional subspace of $\mathcal{H}$ with corresponding Galerkin solution $\widehat{u}_\ell \in \widehat{X}_\ell$. Then, the *$h$-$h/2$-error estimator*

$$\eta_\ell := |||\widehat{u}_\ell - u_\ell||| \tag{3}$$

is a computable quantity which, under suitable conditions, can be used to estimate $|||u-u_\ell|||$. Using the Galerkin orthogonality relation,

$$|||u - u_\ell|||^2 = |||u - \widehat{u}_\ell|||^2 + |||\widehat{u}_\ell - u_\ell|||^2,$$

we infer that η_ℓ is always *efficient*, that is,

$$\eta_\ell \le C_{\text{eff}}\, |||u - u_\ell|||, \tag{4}$$

Date: April 9, 2009.

with constant $C_{\rm eff} = 1$. Moreover, *reliability* of η_ℓ, that is,

$$|||u - u_\ell||| \le C_{\rm rel}\, \eta_\ell, \tag{5}$$

is equivalent to the saturation assumption

$$|||u - \widehat{u}_\ell||| \le C_{\rm sat}\, |||u - u_\ell||| \quad \text{with some uniform constant } C_{\rm sat} \in (0,1). \tag{6}$$

This equivalence is readily verified using the relations $C_{\rm rel} = (1 - C_{\rm sat}^2)^{-1/2}$ and $C_{\rm sat} = (1 - C_{\rm rel}^{-2})^{1/2}$.

To state our adaptive algorithm, we additionally assume that $\mu_\ell(T)$ is a computable quantity which (at least heuristically) measures the local error between the exact solution u and a discrete solution $u_\ell \in X_\ell$ on an element $T \in \mathcal{T}_\ell$. These so-called *refinement indicators* are then used to steer the adaptive mesh-refinement. To link the refinement indicators with η_ℓ, we assume that

$$C_1^{-1}\, \eta_\ell \le \mu_\ell := \Big(\sum_{T \in \mathcal{T}_\ell} \mu_\ell(T)^2 \Big)^{1/2} \le C_2\, \eta_\ell \quad \text{for all } \ell \in \mathbb{N}, \tag{7}$$

with ℓ-independent constants $C_1, C_2 > 0$. The adaptive algorithm then reads as follows:

Algorithm 1. *Let an initial triangulation $\mathcal{T}_0$ with associated discrete space X_0 and an adaptivity parameter $\theta \in (0,1)$ be given. For $\ell = 0, 1, 2, \dots$ do the following:*

(a) *Compute discrete solution $u_\ell \in X_\ell$.*
(b) *Compute refinement indicators $\mu_\ell(T)$ for all $T \in \mathcal{T}_\ell$.*
(c) *Stop, if u_ℓ is sufficiently accurate (e.g., μ_ℓ resp. η_ℓ is sufficiently small).*
(d) *Otherwise, choose a set $\mathcal{M}_\ell \subseteq \mathcal{T}_\ell$ of marked elements such that*

$$\theta \sum_{T \in \mathcal{T}_\ell} \mu_\ell(T)^2 \le \sum_{T \in \mathcal{M}_\ell} \mu_\ell(T)^2. \tag{8}$$

(e) *Refine at least the marked elements $T \in \mathcal{M}_\ell$, generate a new mesh $\mathcal{T}_{\ell+1}$ and an associated discrete space $X_{\ell+1}$, increase the counter $\ell \mapsto \ell + 1$, and go to* (a). □

Note that Algorithm 1, in practice, yields nestedness $X_\ell \subsetneqq X_{\ell+1}$ of the discrete spaces. We denote by X_∞ the closure of $\bigcup_{\ell=0}^\infty X_\ell$ in $\mathcal{H}$. Then, X_∞ is a Hilbert space and thus there is a unique solution $u_\infty \in X_\infty$ of

$$\langle\!\langle u_\infty\, ,\, v_\infty \rangle\!\rangle = F(v_\infty) \quad \text{for all } v_\infty \in X_\infty. \tag{9}$$

As a consequence of Céa's Lemma we obtain the convergence $u_\ell \to u_\infty$ as $\ell \to \infty$ with respect to the energy norm $|||\cdot|||$. In general, however, the adaptive algorithm may lead to $X_\infty \subsetneqq \mathcal{H}$, so that this convergence does not imply $u_\infty = u$.

We say that Algorithm 1 is *convergent* if, and only if, $u_\ell \to u$ as $\ell \to \infty$. In this sense, convergence of an adaptive algorithm has first been proven in [5], where also the marking criterion (8) is introduced. The latter work considered the residual error estimator for a P1-finite element discretization of the Poisson problem, and it is assumed that data oscillations on the initial mesh are sufficiently small. In [11], the resolution of the data oscillations is included into the adaptive algorithm. The convergence analysis is based on reliability and the so-called *discrete local efficiency* of the residual error estimator, which relies on an *interior node property* for the local refinement. The main idea of the convergence proof then is to show that the error is contractive up to the data oscillations. Cascon *et al.* [4]

recently presented a new convergence proof under weaker conditions. They showed that a weighted sum of error and error estimator satisfies a contraction property *without* requiring (discrete local) efficiency of the estimator. In all of the cited works [4, 5, 11], the focus was on residual-based error estimators for conforming finite element schemes.

Our contribution adapts the arguments from [4] to prove that the saturation assumption (6) yields convergence of the adaptive algorithm based on the h-$h/2$-error estimator. Besides the adaptive finite element method (AFEM, Sec. 2), our argument applies to boundary integral formulations and yields a first convergence proof for the adaptive boundary element method (ABEM, Sec. 3). In the case of the finite element method, we combine our arguments with ideas from [11] to show that the h-$h/2$-based version of AFEM leads to convergence even if the saturation assumption fails to hold in general (cf. Sec. 2.6). Numerical experiments in Section 4 conclude the work.

2. Finite Element Method

2.1. Model Problem. We consider the elliptic model problem

$$\begin{aligned} -\Delta u &= f \quad \text{in } \Omega, \\ u &= 0 \quad \text{on } \Gamma_D, \\ \partial_n u &= g \quad \text{on } \Gamma_N. \end{aligned} \tag{10}$$

Here, Ω is a bounded Lipschitz domain in $\mathbb{R}^2$. The boundary Γ is split into a Dirichlet boundary Γ_D and a Neumann boundary Γ_N which satisfy $\Gamma = \overline{\Gamma}_D \cup \overline{\Gamma}_N$ as well as $\Gamma_D \cap \Gamma_N = \emptyset$. Moreover, we assume that Γ_D has positive surface measure $|\Gamma_D| > 0$ so that (10) admits a unique weak solution. The energy scalar product of the weak formulation of (10) reads

$$\langle\!\langle u \,,\, v \rangle\!\rangle := \int_\Omega \nabla u \cdot \nabla v \, dx \quad \text{for all } u, v \in \mathcal{H} = \big\{ u \in H^1(\Omega) \,:\, u|_{\Gamma_D} = 0 \big\}, \tag{11}$$

and the right-hand side is given by

$$F(v) = \int_\Omega f v \, dx + \int_{\Gamma_N} g v \, ds, \tag{12}$$

where ds denotes integration along the boundary. In particular, the energy norm reads $|||v||| = \|\nabla v\|_{L^2(\Omega)}$. We consider the lowest-order Galerkin scheme, where $\mathcal{T}_\ell$ is a regular triangulation of Ω in the sense of Ciarlet and where $X_\ell = \big\{ v_\ell \in \mathcal{S}^1(\mathcal{T}_\ell) \,:\, v_\ell|_{\Gamma_D} = 0 \big\}$ with $\mathcal{S}^1(\mathcal{T}_\ell) = \big\{ v_\ell \in C(\Omega) \,:\, \forall T \in \mathcal{T}_\ell \quad v_\ell|_T \text{ is affine} \big\}$.

To fix notation, $\mathcal{N}_\ell$ denotes the set of nodes of $\mathcal{T}_\ell$, and $\mathcal{E}_\ell$ denotes the set of edges of $\mathcal{T}_\ell$. Moreover, $\mathcal{E}_{N,\ell}$ denotes the set of all edges, which belong to the Neumann boundary Γ_N. The local mesh-width $h_\ell \in L^\infty(\Omega)$ is defined by $h_\ell(x) = \operatorname{diam}(T)$ for $T \in \mathcal{T}_\ell$ and $x \in \operatorname{interior}(T)$. Moreover, $h_\ell(x) = \operatorname{diam}(E)$ if x belongs to the relative interior of an edge $E \in \mathcal{E}_\ell$. Finally, $\mathcal{P}^p(\mathcal{T}_\ell)$ denotes the space of all $\mathcal{T}_\ell$-piecewise polynomials of total degree $\le p$, and $\mathcal{S}^1(\mathcal{T}_\ell) = \mathcal{P}^1(\mathcal{T}_\ell) \cap C(\Omega)$.

2.2. Mesh-Refinement. The essential point in the analysis below is that all sons $T' \in \mathcal{T}_{\ell+1}$ of a marked element $T \in \mathcal{M}_\ell$ also belong to the uniform refinement $\widehat{\mathcal{T}}_\ell$ of $\mathcal{T}_\ell$. We therefore

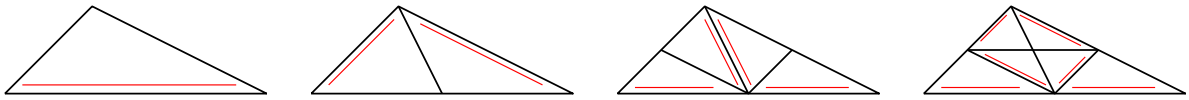

FIGURE 1. For each triangle $T \in \mathcal{T}$, there is one *reference edge*, indicated by the double line (left). Bisection of T is achieved by halving the reference edge, where its midpoint becomes a new node. The reference edges of the son triangles are opposite to this newest vertex (left-middle). Further steps of newest vertex bisection lead to steps, which are denoted by $\mathrm{bisec}_3(T)$ and $\mathrm{bisec}_5(T)$, respectively (right-middle, right).

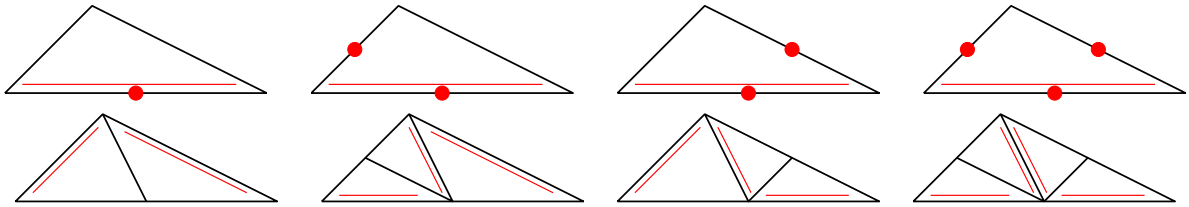

FIGURE 2. Refinement by newest vertex bisection: We consider one triangle T and assume that certain edges, but at least the reference edge, are marked for refinement (top). After refinement, the element is split into 2, 3, or 4 son triangles, respectively (bottom). Throughout, the reference edges are indicated by a double line.

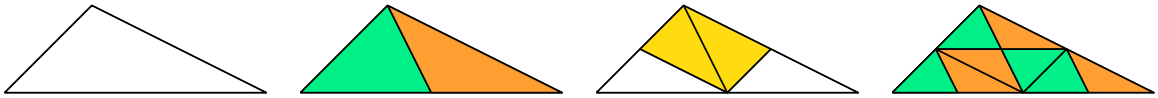

FIGURE 3. Refinement by newest vertex bisection only leads to finitely many interior angles for the family of all possible triangulations obtained by arbitrary newest vertex bisections. To see this, we start from a macro element (left), where the bottom edge is the reference edge. Using iterated newest vertex bisection, one observes that only four similarity classes of triangles occur, which are indicated by the colouring. After three steps of bisections (right), no additional similarity class appears.

generate both meshes $\mathcal{T}_{\ell+1}$ and $\widehat{\mathcal{T}}_\ell$ by the same refinement strategy with respect to the marked elements $\mathcal{M}_\ell$ and $\widehat{\mathcal{M}}_\ell := \mathcal{T}_\ell$, respectively.

Our mesh-refinement is a variant of the newest vertex bisection algorithm (cf. Figure 1), using an edge-based formulation: For a marked element T, we mark all of is edges for refinement. To avoid hanging nodes and to ensure regularity of the refined triangulation, we then proceed recursively: If any edge of an element T' is marked for refinement, we also mark its reference edge. This recursion necessarily terminates after finitely many steps with the result that, for each element in which at least one edge is marked for refinement, the reference edge is marked as well. We then proceed with the refinement rules for newest vertex bisection shown in Figure 2.

However, to guarantee the saturation assumption, we use $\mathrm{bisec}_5(T)$ instead of $\mathrm{bisec}_3(T)$ if an element is marked for refinement, cf. Figure 1. We refer to [6] and the following section

for the fact that uniform bisec$_5$-refinement asymptotically yields the saturation assumption, whereas bisec$_3$ does not.

We stress that refinement rules based on newest vertex bisection ensure the inclusions $X_\ell \subset X_{\ell+1} \subseteq \widehat{X}_\ell \subset \widehat{X}_{\ell+1}$, which are crucial in our analysis. We remark that almost all mesh-refinement strategies will yield $X_\ell \subset X_{\ell+1}$ and $X_\ell \subset \widehat{X}_\ell$. However, the inclusions $X_{\ell+1} \subset \widehat{X}_\ell \subset \widehat{X}_{\ell+1}$ may be violated. For instance, they fail in general for the popular red-green-blue refinement strategies [14].

2.3. Saturation Assumption. In [6], it is stated (without a proof) that the saturation assumption (6) holds for the homogeneous Dirichlet problem (10) with $\Gamma_D = \partial\Omega$, if $\widehat{\mathcal{T}}_\ell$ is obtained by uniform red-refinement of $\mathcal{T}_\ell$ and if data oscillations are sufficiently small. Here, red-refinement means that each triangle $T \in \mathcal{T}_\ell$ is divided into four similar son triangles $T_1, \dots, T_4 \in \widehat{\mathcal{T}}_\ell$. The notion *data oscillations* is understood as

$$\widetilde{\operatorname{osc}}_\ell^2 = \sum_{z \in \mathcal{N}_\ell} \|h_\ell (f - f_{\ell,z})\|^2_{L^2(\omega_{\ell,z})}, \tag{13}$$

where $\omega_{\ell,z} := \bigcup \{T \in \mathcal{T}_\ell : z \in T\}$ is the patch of a node z with respect to $\mathcal{T}_\ell$ and where $f_{\ell,z} := |\omega_{\ell,z}|^{-1} \int_{\omega_{\ell,z}} f\,dx$ denotes the patch-wise integral mean of f.

For $\Gamma_N = \emptyset$ and with bisec$_5$ replacing red-refinement, an analogous result is already contained in [11], although not stated explicitly; compare Equation (14) below and [11, Lemma 4.2]. For the mixed boundary value problem (10), we sketch the proof of the saturation assumption for the convenience of the reader.

Proposition 2. *Let $\widehat{\mathcal{T}}_\ell$ be obtained by uniform bisec$_5$-refinement of $\mathcal{T}_\ell$, and let $u_\ell \in X_\ell$ and $\widehat{u}_\ell \in \widehat{X}_\ell$ be the corresponding Galerkin solutions to* (10)*. Then, there exists a constant $\widetilde{C}_{\rm sat} \in (0,1)$ such that*

$$|||u - \widehat{u}_\ell|||^2 \le \widetilde{C}_{\rm sat}^2 |||u - u_\ell|||^2 + \operatorname{osc}_\ell^2, \tag{14}$$

where the data oscillations are defined by

$$\operatorname{osc}_\ell^2 = \|h_\ell (f - \Pi_\ell f)\|^2_{L^2(\Omega)} + \|h_\ell^{1/2}(g - \Pi_\ell g)\|^2_{L^2(\Gamma_N)}. \tag{15}$$

Here, Π_ℓ denotes the L^2-projection onto $\mathcal{P}^0(\mathcal{T}_\ell)$ and $\mathcal{P}^0(\mathcal{E}_{N,\ell})$, respectively. Consequently, if

$$\operatorname{osc}_\ell^2 \le \lambda\, |||u - u_\ell|||^2, \tag{16}$$

for some $\lambda > 0$ with $C_{\rm sat}^2 = \widetilde{C}_{\rm sat}^2 + \lambda < 1$, then the saturation assumption (6) *is satisfied.*

Sketch of Proof. To prove (14), we consider the residual-based error estimator [14]

$$\varrho_\ell^2 = \sum_{T \in \mathcal{T}_\ell} \varrho_\ell(T)^2$$

with local contributions

$$\varrho_\ell(T)^2 = \|h_\ell f\|^2_{L^2(T)} + \|h_\ell^{1/2}[\partial_n u_\ell]\|^2_{L^2(\partial T \cap \Omega)} + \|h_\ell^{1/2}(g - \partial_n u_\ell)\|^2_{L^2(\partial T \cap \Gamma_N)},$$

where $[\cdot]$ denotes the jump over an interior edge $E \in \mathcal{E}_\ell$. It is well-known that ϱ_ℓ is reliable,

$$|||u - u_\ell||| \le \widetilde{C}_{\rm rel}\, \varrho_\ell. \tag{17}$$

and locally efficient up to oscillation terms,

$$\varrho_\ell(T)^2 \le \widetilde{C}_{\rm eff}^2 \big(\|\nabla(u-u_\ell)\|_{L^2(\omega_T)}^2 + \|h_\ell(f-\Pi_\ell f)\|_{L^2(\omega_T)}^2 + \|h_\ell^{1/2}(g-\Pi_\ell g)\|_{L^2(\partial T\cap\Gamma_N)}^2\big), \tag{18}$$

where $\omega_T = \{T\} \cup \bigcup \{T' \in \mathcal{T}_\ell : T \cap T' \in \mathcal{E}_\ell\}$ denotes the element patch of $T \in \mathcal{T}_\ell$, cf. [14]. The proof of (18) goes back to Verfürth [13] and is obtained by use of appropriate bubble functions. First,

$$\|h_\ell \Pi_\ell f\|_{L^2(T)} \lesssim \|\nabla u - \nabla u_\ell\|_{L^2(T)} + \|h_\ell(f-\Pi_\ell f)\|_{L^2(T)} \tag{19}$$

follows by use of the element bubble $b_T \in \mathcal{P}^3(T) \cap H^1_0(T)$. Second, for an interior edge $E \in \mathcal{E}_\ell$, let $E = T \cap T'$ and denote by $\omega_E = T \cup T'$ the corresponding edge patch. Then, by use of the edge bubble $b_E \in \mathcal{P}^2(\{T,T'\}) \cap H^1_0(\omega_E)$, one can prove that

$$\|h_\ell^{1/2}[\partial_n u_\ell]\|_{L^2(E)} \lesssim \|\nabla u - \nabla u_\ell\|_{L^2(\omega_E)} + \|h_\ell f\|_{L^2(\omega_E)}. \tag{20}$$

Third, for a Neumann edge $E \in \mathcal{E}_{N,\ell}$ with corresponding element $T \in \mathcal{T}_\ell$, using again the edge bubble $b_E \in \mathcal{P}^2(T)$ with $b_E|_{\partial T\setminus E} = 0$, one shows that

$$\|h_\ell^{1/2}(\Pi_\ell g - \partial_n u_\ell)\|_{L^2(E)} \lesssim \|\nabla u - \nabla u_\ell\|_{L^2(T)} + \|h_\ell f\|_{L^2(T)} + \|h_\ell^{1/2}(g-\Pi_\ell g)\|_{L^2(E)}. \tag{21}$$

Using the triangle inequality and (19)–(21), one obtains (18).

In all of the three estimates (19)–(21), the term ∇u on the right-hand side stems from the weak form (1) applied with the properly weighted bubble functions $v \in \{b_T, b_E\}$. It has already been observed by Dörfler [5] that one may use the hat function $v = b_E \in \widehat{X}_\ell$ for the midpoint of an edge $E \in \mathcal{E}_\ell$ instead of the edge bubble function. This allows to use the Galerkin formulation (2) for $\widehat{X}_\ell$ instead of the continuous variational form (1) and leads to $\nabla\widehat{u}_\ell$ instead of ∇u in (20)–(21). Finally, it was noticed in [11] that one may use the hat function $v = b_T \in \widehat{X}_\ell$ which corresponds to the interior node of $\mathrm{bisec}_5(T)$ instead of the element bubble, cf. Figure 1. This leads to $\nabla\widehat{u}_\ell$ instead of ∇u in (19). With these two observations, one can therefore use Verfürth's proof to verify the local discrete efficiency

$$\varrho_\ell(T)^2 \le \widetilde{C}_{\rm eff}^2\big(\|\nabla(\widehat{u}_\ell-u_\ell)\|_{L^2(\omega_T)}^2 + \|h_\ell(f-\Pi_\ell f)\|_{L^2(\omega_T)}^2 + \|h_\ell^{1/2}(g-\Pi_\ell g)\|_{L^2(\partial T\cap\Gamma_N)}^2\big), \tag{22}$$

for all $T \in \mathcal{T}_\ell$, even with the same constant as in (18). Summation over all elements $T \in \mathcal{T}_\ell$ results in

$$\varrho_\ell^2 \le 3\widetilde{C}_{\rm eff}^2\big(|||\widehat{u}_\ell - u_\ell|||^2 + \mathrm{osc}_\ell^2\big) \tag{23}$$

since each element $T \in \mathcal{T}_\ell$ is at most counted three times.

Now, we are in a position to verify (14): The combination of (17) and (23) yields

$$|||u-u_\ell|||^2 \le \widetilde{C}_{\rm rel}^2\,\varrho_\ell^2 \le 3\widetilde{C}_{\rm eff}^2\widetilde{C}_{\rm rel}^2\big(|||\widehat{u}_\ell-u_\ell|||^2 + \mathrm{osc}_\ell^2\big).$$

With $C := 3\widetilde{C}_{\rm eff}^2\widetilde{C}_{\rm rel}^2$, the Galerkin orthogonalities for $\widehat{X}_\ell$ and $X_\ell \subset \widehat{X}_\ell$ prove

$$|||u-\widehat{u}_\ell|||^2 = |||u-u_\ell|||^2 - |||\widehat{u}_\ell-u_\ell|||^2 \le (C-1)|||\widehat{u}_\ell-u_\ell|||^2 + C\,\mathrm{osc}_\ell^2.$$

Thus, a further application of the Galerkin orthogonality yields

$$C\,|||u-\widehat{u}_\ell|||^2 \le (C-1)|||u-u_\ell|||^2 + C\,\mathrm{osc}_\ell^2$$

and concludes the proof with $\widetilde{C}_{\rm sat}^2 = (C-1)/C$. □

2.4. Refinement Indicators. In this section, we discuss the refinement indicators

$$\widetilde{\mu}_\ell(T) = \|\nabla\widehat{u}_\ell - \Pi_\ell(\nabla\widehat{u}_\ell)\|_{L^2(T)} \quad \text{and} \quad \mu_\ell(T) = \|\nabla(\widehat{u}_\ell - I_\ell\widehat{u}_\ell)\|_{L^2(T)}, \tag{24}$$

as well as

$$\eta_\ell(T) = \|\nabla\widehat{u}_\ell - \nabla u_\ell\|_{L^2(T)}. \tag{25}$$

Here, $\Pi_\ell : L^2(\Omega) \to \mathcal{P}^0(\mathcal{T}_\ell)^2$ denotes the L^2-projection onto the $\mathcal{T}_\ell$-piecewise constant fields, and $I_\ell : C(\overline{\Omega}) \to X_\ell$ denotes the nodal interpolation operator. Since Π_ℓ is even the $\mathcal{T}_\ell$-piecewise orthogonal projection and $\nabla u_\ell \in \mathcal{P}^0(\mathcal{T}_\ell)^2$, it holds that

$$\widetilde{\mu}_\ell(T) \le \mu_\ell(T) \quad \text{and} \quad \widetilde{\mu}_\ell(T) \le \eta_\ell(T) \qquad \text{for all } T \in \mathcal{T}_\ell. \tag{26}$$

Together with the best approximation property of the Galerkin solution $u_\ell \in X_\ell$, this provides the global estimates

$$\widetilde{\mu}_\ell = \|\nabla\widehat{u}_\ell - \Pi_\ell(\nabla\widehat{u}_\ell)\|_{L^2(\Omega)} \le \eta_\ell \le \mu_\ell = \|\nabla(\widehat{u}_\ell - I_\ell\widehat{u}_\ell)\|_{L^2(\Omega)}. \tag{27}$$

The following proposition states the converse inequalities.

Proposition 3. *There is a constant $C_3 \ge 1$ which only depends on the smallest interior angle in $\mathcal{T}_\ell$ such that*

$$\mu_\ell(T) \le C_3\,\widetilde{\mu}_\ell(T) \quad \textit{for all } T \in \mathcal{T}_\ell, \tag{28}$$

so that

$$C_3^{-1}\mu_\ell \le \widetilde{\mu}_\ell \le \eta_\ell \le \mu_\ell \tag{29}$$

In particular, the error estimators η_ℓ, $\widetilde{\mu}_\ell$, and μ_ℓ are equivalent in the sense of (7).

Proof. Let C_∞ denote an upper bound on the norm of the interpolation operator I_ℓ in the $W^{1,\infty}$-semi-norm, valid in each element $T \in \mathcal{T}_\ell$, more precisely, we require

$$\|\nabla(I_\ell\widehat{v}_\ell)\|_{L^\infty(T)} \le C_\infty\|\nabla\widehat{v}_\ell\|_{L^\infty(T)} \qquad \text{for all } \widehat{v}_\ell \in \widehat{X}_\ell \quad \text{and } T \in \mathcal{T}_\ell.$$

We note that, for rectangular elements, $C_\infty = 1$. It is clear that, in general, the constant is bounded only in terms of the mesh quality.

Furthermore, we note that our refinement strategy yields a uniform constant $\rho > 0$ so that $|T'| \ge \rho|T|$ whenever T' is a son of T. Let v be an affine function defined on T with gradient $\nabla v = \Pi_\ell\widehat{u}_\ell$, then

$$\begin{aligned}
\|\nabla(1 - I_\ell)\widehat{u}_\ell\|^2_{L^2(T)} &= \|(1 - \Pi_\ell)\nabla(1 - I_\ell)\widehat{u}_\ell\|^2_{L^2} + \|\Pi_\ell\nabla(1 - I_\ell)\widehat{u}_\ell\|^2_{L^2(T)} \\
&= \widetilde{\mu}_\ell(T)^2 + \|\nabla v - \nabla I_\ell\widehat{u}_\ell\|^2_{L^2(T)} \\
&\le \widetilde{\mu}_\ell(T)^2 + |T|C_\infty^2\|\nabla v - \nabla\widehat{u}_\ell\|^2_{L^\infty(T)} \\
&\le \widetilde{\mu}_\ell(T)^2 + \rho^{-1}C_\infty^2 \sum_{T' \subset T} |T'|\|(\Pi_\ell - 1)\nabla\widehat{u}_\ell\|^2_{L^\infty(T')} \\
&= (1 + \rho^{-1}C_\infty^2)\widetilde{\mu}_\ell(T)^2.
\end{aligned}$$

This establishes (28) with $C_3 = (1 + \rho^{-1}C_\infty^2)^{1/2}$. □

2.5. Convergence of AFEM under the Saturation Assumption. We first prove convergence of the adaptive finite element scheme, based on the refinement indicators $\widetilde{\mu}_\ell(T)$ from (24).

Theorem 4. *Suppose that we use the indicators $\widetilde{\mu}_\ell(T)$, defined in (24), in Algorithm 1. Under the saturation assumption (6) and for any choice of $\theta \in (0,1)$, there are constants $\kappa, \gamma \in (0,1)$ such that*

$$\widetilde{\Delta}_\ell := |||u - u_\ell|||^2 + |||u - \widehat{u}_\ell|||^2 + \gamma\, \widetilde{\mu}_\ell^2 \tag{30}$$

satisfies the contraction property

$$\widetilde{\Delta}_{\ell+1} \le \kappa \widetilde{\Delta}_\ell. \tag{31}$$

In particular, it holds that $\lim_{\ell\to\infty} |||u - \widehat{u}_\ell||| = \lim_{\ell\to\infty} |||u - u_\ell||| = 0 = \lim_{\ell\to\infty} \widetilde{\mu}_\ell$.

Proof. Application of the triangle inequality yields

$$\begin{aligned}
\widetilde{\mu}_{\ell+1} &= \|(1-\Pi_{\ell+1})(\nabla\widehat{u}_{\ell+1})\|_{L^2(\Omega)} \\
&\le \|(1-\Pi_{\ell+1})(\nabla\widehat{u}_\ell)\|_{L^2(\Omega)} + \|(1-\Pi_{\ell+1})(\nabla\widehat{u}_{\ell+1} - \nabla\widehat{u}_\ell)\|_{L^2(\Omega)} \\
&\le \|\nabla\widehat{u}_\ell - \Pi_{\ell+1}(\nabla\widehat{u}_\ell)\|_{L^2(\Omega)} + \|\nabla\widehat{u}_{\ell+1} - \nabla\widehat{u}_\ell\|_{L^2(\Omega)},
\end{aligned}$$

where we have used orthogonality of $\Pi_{\ell+1}$ in the final estimate. According to the mesh-refinement rule from Section 2.2, and since ∇u_ℓ is constant on the six sons $T' \in \mathcal{T}_{\ell+1} \cap \widehat{\mathcal{T}}_\ell$ of $T \in \mathcal{M}_\ell$, it holds that

$$\|\nabla\widehat{u}_\ell - \Pi_{\ell+1}(\nabla\widehat{u}_\ell)\|_{L^2(T)} = 0 \quad \text{for all } T \in \mathcal{M}_\ell.$$

Moreover, $\mathcal{T}_{\ell+1}$-piecewise orthogonality of $\Pi_{\ell+1}$ yields

$$\|\nabla\widehat{u}_\ell - \Pi_{\ell+1}(\nabla\widehat{u}_\ell)\|_{L^2(T)} \le \|\nabla\widehat{u}_\ell - \Pi_\ell(\nabla\widehat{u}_\ell)\|_{L^2(T)} = \widetilde{\mu}_\ell(T) \quad \text{for all } T \in \mathcal{T}_\ell \backslash \mathcal{M}_\ell.$$

Finally, Dörfler's marking strategy (8) provides

$$\sum_{T\in\mathcal{T}_\ell\backslash\mathcal{M}_\ell} \widetilde{\mu}_\ell(T)^2 = \widetilde{\mu}_\ell^2 - \sum_{T\in\mathcal{M}_\ell} \widetilde{\mu}_\ell(T)^2 \le (1-\theta)\widetilde{\mu}_\ell^2. \tag{32}$$

The combination of the three foregoing observations reads

$$\|\nabla\widehat{u}_\ell - \Pi_{\ell+1}(\nabla\widehat{u}_\ell)\|_{L^2(\Omega)}^2 = \sum_{T\in\mathcal{T}_\ell\backslash\mathcal{M}_\ell} \|\nabla\widehat{u}_\ell - \Pi_{\ell+1}(\nabla\widehat{u}_\ell)\|_{L^2(T)}^2 \le \sum_{T\in\mathcal{T}_\ell\backslash\mathcal{M}_\ell} \widetilde{\mu}_\ell(T)^2 \le \varrho\, \widetilde{\mu}_\ell^2$$

with $\varrho := 1-\theta < 1$. For any $\delta > 0$, Young's inequality thus proves

$$\widetilde{\mu}_{\ell+1}^2 \le (1+\delta)\varrho\, \widetilde{\mu}_\ell^2 + (1+\delta^{-1})|||\widehat{u}_{\ell+1} - \widehat{u}_\ell|||^2.$$

To abbreviate the notation, we define $e_\ell := |||u - u_\ell|||^2$ and $E_\ell := |||u_{\ell+1} - u_\ell|||^2$ as well as $\widehat{e}_\ell := |||u - \widehat{u}_\ell|||^2$ and $\widehat{E}_\ell := |||\widehat{u}_{\ell+1} - \widehat{u}_\ell|||^2$. Since $\mathcal{T}_{\ell+1}$ is obtained by refinement of $\mathcal{T}_\ell$ it holds that $X_\ell \subsetneqq X_{\ell+1}$, and therefore, Galerkin orthogonality implies that $e_{\ell+1} + E_\ell = e_\ell$. Similarly, since $\widehat{X}_\ell \subsetneqq \widehat{X}_{\ell+1}$, we also have $\widehat{e}_{\ell+1} + \widehat{E}_\ell = \widehat{e}_\ell$. With this notation, the last inequality can be rewritten as

$$\widetilde{\mu}_{\ell+1}^2 \le (1+\delta)\varrho\, \widetilde{\mu}_\ell^2 + C_\delta(E_\ell + \widehat{E}_\ell), \tag{33}$$

where $C_\delta = (1+\delta^{-1})$. The additional term E_ℓ will appear for the adaptive boundary element schemes discussed below, hence we already include it in our present analysis.

We now choose $\delta > 0$ such that $(1+\delta)\varrho < 1$. Next, we choose $\gamma \in (0,1)$ such that $\gamma C_\delta \le 1$. Then, Galerkin orthogonality and choice of γ prove

$$\widetilde{\Delta}_{\ell+1} = e_{\ell+1} + \widehat{e}_{\ell+1} + \gamma\widetilde{\mu}_{\ell+1}^2 = e_\ell + \widehat{e}_\ell - (E_\ell + \widehat{E}_\ell) + \gamma\widetilde{\mu}_{\ell+1}^2 \le e_\ell + \widehat{e}_\ell + \gamma(1+\delta)\varrho\, \widetilde{\mu}_\ell^2. \tag{34}$$

Note that so far only the last term on the right-hand side is contractive. Therefore, we choose an additional parameter $\beta > 0$ with $\beta + (1+\delta)\varrho < 1$ and write

$$e_\ell + \gamma(1+\delta)\varrho\,\widetilde{\mu}_\ell^2 = (e_\ell - \gamma\beta\widetilde{\mu}_\ell^2) + \gamma[\beta + (1+\delta)\varrho]\,\widetilde{\mu}_\ell^2.$$

Recall that the saturation assumption (6) is equivalent to the reliability (5) of the h-$h/2$ error estimator η_ℓ. Thus, the equivalence (7) of η_ℓ and $\widetilde{\mu}_\ell$ proves reliability of $\widetilde{\mu}_\ell$, i.e. $e_\ell = |||u - u_\ell|||^2 \le C_4\,\widetilde{\mu}_\ell^2$, and hence

$$\widetilde{\Delta}_{\ell+1} \le (1 - \gamma\beta C_4^{-1})e_\ell + \widehat{e}_\ell + \gamma[\beta + (1+\delta)\varrho]\,\widetilde{\mu}_\ell^2.$$

Finally, we choose $\varepsilon > 0$ so that $\varepsilon < \gamma\beta C_4^{-1}$. Since $\widehat{e}_\ell \le e_\ell$, we obtain

$$\widetilde{\Delta}_{\ell+1} \le (1 - \gamma\beta C_4^{-1} + \varepsilon)e_\ell + (1-\varepsilon)\widehat{e}_\ell + \gamma[\beta + (1+\delta)\varrho]\,\widetilde{\mu}_\ell^2 \le \kappa\widetilde{\Delta}_\ell,$$

where $\kappa = \max\big\{\, 1 - \gamma\beta C_4^{-1} + \varepsilon\,,\, 1 - \varepsilon\,,\, \beta + (1+\delta)\varrho \,\big\} < 1$. □

Remark. *Note that, in view of* (34) *and* $(1+\delta)\varrho < 1$*, the error quantity* $\widetilde{\Delta}_\ell$ *is monotonically decreasing, i.e.* $\widetilde{\Delta}_{\ell+1} \le \widetilde{\Delta}_\ell$*, even if the saturation assumption fails to hold.* □

Remark. *We stress that only the estimator reduction* (33) *depends on the precise mathematical setting as well as on the refinement indicators chosen. The remainder of the proof works in a general framework so that we shall only verify* (33) *in the following, whenever we aim to prove convergence by verification of a contraction property for some error quantity.* □

Next, we observe that the previous theorem also implies convergence of the μ_ℓ-based AFEM. We stress that the following result is weaker than Theorem 4 in the sense that the latter provides a contraction property (31) for some error quantity $\widetilde{\Delta}_\ell = |||u - u_\ell|||^2 + |||u - \widehat{u}_\ell|||^2 + \gamma\widetilde{\mu}_\ell^2$ which then necessarily satisfies $\lim_\ell \widetilde{\Delta}_\ell = 0$. In contrast, the following result only states $\lim_\ell \Delta_\ell = 0$, where $\Delta_\ell = |||u - u_\ell|||^2 + |||u - \widehat{u}_\ell|||^2 + \gamma\,\mu_\ell^2$. The contraction property of Δ_ℓ is only proven for sufficiently large $\theta \in (0,1)$. This, however, seems to be suboptimal: We stress that $\theta = 1$ generically leads to uniform mesh-refinement, whereas small $\theta \ll 1$ yields highly adapted meshes.

Theorem 5. *Suppose that we use the indicators* $\mu_\ell(T)$ *defined in* (24) *in Algorithm 1, and assume that the saturation assumption* (6) *holds. Then, for any choice of* $\theta \in (0,1)$*,*

$$\lim_{\ell\to\infty} |||u - \widehat{u}_\ell||| = \lim_{\ell\to\infty} |||u - u_\ell||| = 0 = \lim_{\ell\to\infty} \mu_\ell. \tag{35}$$

Provided that $\theta \in (0,1)$ *is sufficiently large, there are constants* $\kappa, \gamma \in (0,1)$ *such that the weighted error quantity*

$$\Delta_\ell := |||u - u_\ell|||^2 + |||u - \widehat{u}_\ell|||^2 + \gamma\,\mu_\ell^2 \tag{36}$$

satisfies the contraction property

$$\Delta_{\ell+1} \le \kappa\Delta_\ell. \tag{37}$$

Proof of Theorem 5 (Convergence). From (28)–(29), we infer

$$\sum_{T\in\mathcal{M}_\ell} \mu_\ell(T)^2 \le C_3 \sum_{T\in\mathcal{M}_\ell} \widetilde{\mu}_\ell(T)^2 \quad \text{as well as} \quad \widetilde{\mu}_\ell^2 \le \mu_\ell^2$$

with some constant $C_3 \ge 1$. Therefore, μ_ℓ-based Dörfler marking (8) with constant $\theta \in (0,1)$ implies $\widetilde{\mu}_\ell$-based Dörfler marking with constant $\widetilde{\theta} = \theta/C_3 \in (0,1)$, namely

$$\theta\widetilde{\mu}_\ell^2 \le \theta\mu_\ell^2 \le \sum_{T\in\mathcal{M}_\ell} \mu_\ell(T)^2 \le C_3 \sum_{T\in\mathcal{M}_\ell} \widetilde{\mu}_\ell(T)^2.$$

Therefore, Theorem 4 implies that $\lim_\ell |||u - \widehat{u}_\ell||| = \lim_\ell |||u - u_\ell||| = 0 = \lim_\ell \widetilde{\mu}_\ell$. From the equivalence of $\widetilde{\mu}_\ell$ and μ_ℓ, we obtain $\lim_\ell \mu_\ell = 0$. □

Proof of Theorem 5 (Contraction Property). A scaling argument with respect to $\mathcal{T}_\ell$ and continuity of $I_{\ell+1}$ onto the finite dimensional space $\widehat{X}_{\ell+1}$ provide some constant $C_5 > 0$ with

$$\|\nabla I_{\ell+1}(\widehat{u}_{\ell+1} - \widehat{u}_\ell)\|_{L^2(T)} \le C_5 \, \|\nabla(\widehat{u}_{\ell+1} - \widehat{u}_\ell)\|_{L^2(T)} \quad \text{for all } T \in \mathcal{T}_\ell.$$

The triangle inequality thus yields

$$\begin{aligned}\mu_{\ell+1} = |||\widehat{u}_{\ell+1} - I_{\ell+1}\widehat{u}_{\ell+1}||| &\le |||\widehat{u}_{\ell+1} - \widehat{u}_\ell||| + |||\widehat{u}_\ell - I_{\ell+1}\widehat{u}_\ell||| + |||I_{\ell+1}(\widehat{u}_{\ell+1} - \widehat{u}_\ell)||| \\ &\le |||\widehat{u}_\ell - I_{\ell+1}\widehat{u}_\ell||| + (C_5+1)\,|||\widehat{u}_{\ell+1} - \widehat{u}_\ell|||.\end{aligned}$$

Copying the proof of Proposition 3 verbatim, we obtain a constant C_6 such that

$$\|\nabla(\widehat{u}_\ell - I_{\ell+1}\widehat{u}_\ell)\|_{L^2(T)} \le C_6 \|\nabla\widehat{u}_\ell - \Pi_{\ell+1}(\nabla\widehat{u}_\ell)\|_{L^2(T)},$$

and in particular,

$$C_6^{-1}\,\|\nabla(\widehat{u}_\ell - I_{\ell+1}\widehat{u}_\ell)\|_{L^2(T)} \le \|\nabla\widehat{u}_\ell - \Pi_\ell(\nabla\widehat{u}_\ell)\|_{L^2(T)} = \widetilde{\mu}_\ell(T) \quad \text{for all } T \in \mathcal{T}_\ell. \tag{38}$$

From $\widetilde{\mu}_\ell(T) \le \mu_\ell(T)$, we thus infer

$$\|\nabla(\widehat{u}_\ell - I_{\ell+1}\widehat{u}_\ell)\|_{L^2(T)} \le C_6\,\mu_\ell(T) \quad \text{for all } T \in \mathcal{T}_\ell.$$

The refinement strategy gives

$$\|\nabla(\widehat{u}_\ell - I_{\ell+1}\widehat{u}_\ell)\|_{L^2(T)} = 0 \quad \text{for all } T \in \mathcal{M}_\ell.$$

The combination of the latter two estimates proves

$$|||\widehat{u}_\ell - I_{\ell+1}\widehat{u}_\ell|||^2 = \sum_{T\in\mathcal{T}_\ell\setminus\mathcal{M}_\ell} \|\nabla(\widehat{u}_\ell - I_{\ell+1}\widehat{u}_\ell)\|_{L^2(T)}^2 \le C_6^2 \sum_{T\in\mathcal{T}_\ell\setminus\mathcal{M}_\ell} \mu_\ell(T)^2 \le C_6^2(1-\theta)\,\mu_\ell^2,$$

where the final estimate follows from the Dörfler marking, cf. (32). We assume that $\theta \in (0,1)$ is sufficiently large to guarantee $\varrho = C_6^2(1-\theta) < 1$. Using the same notation as in the proof of Theorem 4, we obtain the estimator reduction (33) with $C_\delta = (1+\delta^{-1})(C_5+1)^2$. □

From a conceptual point of view, it seems more natural to consider the local contributions $\eta_\ell(T)$ of $\eta_\ell = |||\widehat{u}_\ell - u_\ell|||$ — instead of $\widetilde{\mu}_\ell(T)$ — for marking in step (d) of Algorithm 1. We stress, however, that an adaptive algorithm will usually return $\widehat{u}_\ell$ instead of u_ℓ since $|||u - \widehat{u}_\ell||| \le |||u - u_\ell|||$. One advantage of $\widetilde{\mu}_\ell$ and μ_ℓ from (24) over $\eta_\ell(T)$ now is that we do not need to compute the coarse-mesh solution $u_\ell \in X_\ell$. Instead, $\Pi_\ell(\nabla\widehat{u}_\ell)$, for instance, can simply be computed in linear complexity by $\Pi_\ell(\nabla\widehat{u}_\ell)|_T = (1/|T|)\int_T \nabla\widehat{u}_\ell\,dx$, for all $T \in \mathcal{T}_\ell$.

Remark. *Although numerical experiments give evidence that the steering of Algorithm 1 by $\eta_\ell(T)$ leads to a convergent adaptive scheme, we did not succeed to prove convergence for arbitrary but only for* sufficiently large $\theta \in (0,1)$.

For example, closely following the proof of the contraction property in Theorem 5 one can show that, if $(1-\theta)C_6^2 < 1$, then the combined error quantity

$$\overline{\Delta}_\ell := |||u - u_\ell|||^2 + |||u - \widehat{u}_\ell|||^2 + \gamma\, \eta_\ell^2$$

satisfies a contraction property. □

2.6. Convergence of AFEM without the Saturation Assumption. In this section, we include the resolution of the data oscillations into the adaptive algorithm. With

$$\operatorname{osc}_\ell(T)^2 = \|h_\ell(f - \Pi_\ell f)\|_{L^2(T)}^2 + \|h_\ell^{1/2}(g - \Pi_\ell g)\|_{L^2(\partial T \cap \Gamma_N)}^2, \tag{39}$$

we consider

$$\widetilde{\zeta}_\ell^2 = \sum_{T \in \mathcal{T}_\ell} \widetilde{\zeta}_\ell(T)^2 = \widetilde{\mu}_\ell^2 + \operatorname{osc}_\ell^2, \quad \text{where} \quad \widetilde{\zeta}_\ell(T)^2 = \widetilde{\mu}_\ell(T)^2 + \operatorname{osc}_\ell(T)^2. \tag{40}$$

By use of Proposition 2, we will show that this estimator enforces the saturation assumption to hold. The following theorem states convergence of the $\widetilde{\zeta}_\ell$-based version of AFEM.

Theorem 6. *Suppose that we use the indicators $\widetilde{\zeta}_\ell(T)$ defined in* (40) *in Algorithm 1. Then, for any $\theta \in (0,1)$, there is a constant $\gamma \in (0,1)$ such that the combined error quantity*

$$\widetilde{Z}_\ell := |||u - u_\ell|||^2 + |||u - \widehat{u}_\ell|||^2 + \gamma\, \widetilde{\zeta}_\ell^2$$

satisfies $\lim_{\ell\to\infty} \widetilde{Z}_\ell = 0$. In particular, it holds that $\lim_{\ell\to\infty} |||u - \widehat{u}_\ell||| = \lim_{\ell\to\infty} |||u - u_\ell||| = 0 = \lim_{\ell\to\infty} \widetilde{\zeta}_\ell$.

Proof. Note that the data oscillations satisfy

$$\operatorname{osc}_{\ell+1}(T)^2 \le \operatorname{osc}_\ell(T)^2 \quad \text{for } T \in \mathcal{T}_\ell, \quad \text{as well as} \quad \operatorname{osc}_{\ell+1}(T)^2 \le \frac{1}{2}\operatorname{osc}_\ell(T)^2 \quad \text{for } T \in \mathcal{M}_\ell.$$

In particular, the data oscillations are monotonically decreasing. With the same arguments as, e.g., in the proof of Theorem 4 above, we thus obtain the estimator reduction

$$\widetilde{\zeta}_{\ell+1}^2 \le (1+\delta)\varrho\, \widetilde{\zeta}_\ell^2 + 4(1+\delta^{-1})|||\widehat{u}_{\ell+1} - \widehat{u}_\ell|||^2 \tag{41}$$

with $\varrho = 1 - \theta/2$, for all $\delta > 0$. Arguing as above, we find $\gamma \in (0,1)$ such that $\widetilde{Z}_\ell$ is monotonically decreasing, i.e. $\widetilde{Z}_{\ell+1} \le \widetilde{Z}_\ell$. Moreover, the saturation assumption

$$C_\ell := \frac{|||u - \widehat{u}_\ell|||}{|||u - u_\ell|||} < 1$$

in the ℓ-step implies contraction $\widetilde{Z}_{\ell+1} \le \kappa_\ell \widetilde{Z}_\ell$ for some $\kappa_\ell \in (0,1)$, which depends on C_ℓ and which satisfies $\kappa_\ell \to 1$ if and only if $C_\ell \to 1$ as $\ell \to \infty$.

Provided that $\liminf_\ell C_\ell < 1$, the according subsequence thus satisfies $1 > \kappa \ge \kappa_{\ell_k}$. Therefore, monotonicity of $\widetilde{Z}_\ell$ yields $\widetilde{Z}_{\ell_{k+1}} \le \widetilde{Z}_{\ell_k+1} \le \kappa\, \widetilde{Z}_{\ell_k}$, whence $\lim_k \widetilde{Z}_{\ell_k} = 0$. Again by monotonicity of $\widetilde{Z}_\ell$, the whole sequence satisfies $\lim_\ell \widetilde{Z}_\ell = 0$.

We may thus restrict to consider the case $\lim_\ell C_\ell = \liminf_\ell C_\ell = 1$. Note that the Galerkin orthogonality $|||u - \widehat{u}_\ell|||^2 + \eta_\ell^2 = |||u - u_\ell|||^2$ then implies $\lim_\ell \eta_\ell^2 = 0$, hence $\lim_\ell \widetilde{\mu}_\ell^2 = 0$. For

$\varepsilon > 0$, we choose a sufficiently large ℓ_0 such that $\widetilde{\mu}_\ell^2 \le \varepsilon$ for all $\ell \ge \ell_0$. Dörfler's marking strategy provides

$$\begin{aligned}\operatorname{osc}_{\ell+1}^2 \le \sum_{T\in\mathcal{T}_\ell\setminus\mathcal{M}_\ell} \operatorname{osc}_\ell(T)^2 + \frac{1}{2}\sum_{T\in\mathcal{M}_\ell} \operatorname{osc}_\ell(T)^2 &= \operatorname{osc}_\ell^2 - \frac{1}{2}\sum_{T\in\mathcal{M}_\ell} \widetilde{\zeta}_\ell(T)^2 + \frac{1}{2}\sum_{T\in\mathcal{M}_\ell} \widetilde{\mu}_\ell(T)^2 \\ &\le \operatorname{osc}_\ell^2 - \frac{\theta}{2}\,\widetilde{\zeta}_\ell^2 + \frac{1}{2}\sum_{T\in\mathcal{M}_\ell} \widetilde{\mu}_\ell(T)^2 \\ &\le (1-\theta/2)\operatorname{osc}_\ell^2 + \varepsilon/2.\end{aligned}$$

By induction, the geometric series provides

$$\operatorname{osc}_{\ell+k}^2 \le (1-\theta/2)^k \operatorname{osc}_\ell^2 + (\varepsilon/2)\sum_{j=1}^{k}(1-\theta/2)^j \le (1-\theta/2)^k \operatorname{osc}_0^2 + \varepsilon/\theta,$$

where we have used the monotonicity of data oscillations $\operatorname{osc}_{\ell+1}^2 \le \operatorname{osc}_\ell^2$. From this, we infer $\limsup_\ell \operatorname{osc}_\ell^2 \le \varepsilon/\theta$ for all $\varepsilon > 0$ and conclude $\lim_\ell \operatorname{osc}_\ell^2 = 0$. Due to $|||u - \widehat{u}_\ell||| \le |||u - u_\ell|||$ and $\lim_\ell \widetilde{\zeta}_\ell^2 = 0$, the estimate $\widetilde{Z}_\ell > C > 0$ then implies $|||u - u_\ell|||^2 \ge C/2$. In particular, Proposition 2 implies that the saturation assumption holds for all $\ell \ge \ell_0$, as soon as $\operatorname{osc}_{\ell_0}^2 \le \lambda C/4$. This, however, contradicts $\lim_\ell C_\ell = 1$ and thus proves $\lim_\ell \widetilde{Z}_\ell = 0$. □

Remark. *Using the arguments of Theorem 5 above, one may prove that, for arbitrary $\theta \in (0,1)$, the indicators $\zeta_\ell(T)^2 := \mu_\ell(T)^2 + \operatorname{osc}_\ell(T)^2$ also lead to a convergent version of AFEM.* □

3. Boundary Element Method

3.1. Symm's Integral Equation. As model problem, we consider the first-kind integral equation

$$(Vu)(x) = \int_\Gamma G(x,y)u(y)\,ds_y = F(x) \quad \text{for } x \in \Gamma \tag{42}$$

with the weakly-singular integral kernel

$$G(x,y) = \begin{cases} -\dfrac{1}{2\pi}\,\log|x-y| & \text{for } d = 2, \\ +\dfrac{1}{4\pi}\,\dfrac{1}{|x-y|} & \text{for } d = 3. \end{cases} \tag{43}$$

Here, Γ is an open piece of the boundary $\partial\Omega$ of a Lipschitz domain Ω in $\mathbb{R}^d$, and ds denotes the integration along the arclength or on the manifold for $d = 2, 3$, respectively. For $d = 2$, we additionally assume $\operatorname{diam}(\Omega) < 1$. We define the fractional-order Sobolev space

$$H^{1/2}(\Gamma) := \{\widetilde{u}|_\Gamma \,|\, \widetilde{u} \in H^1(\Omega)\}$$

with norm

$$\|u\|_{H^{1/2}(\Gamma)} := \inf\big\{\|\widetilde{u}\|_{H^1(\Omega)} \,\big|\, \widetilde{u} \in H^1(\Omega) \text{ with } \widetilde{u}|_\Gamma = u\big\}.$$

Then, $H^{1/2}(\Gamma)$ is a Hilbert space, and we define $\widetilde{H}^{-1/2}(\Gamma)$ as the algebraic-topological dual of $H^{1/2}(\Gamma)$ with respect to the extended L^2-scalar product $\langle\cdot\,,\,\cdot\rangle$. The single-layer potential V is an elliptic isomorphism between $\mathcal{H} = \widetilde{H}^{-1/2}(\Gamma)$ and $H^{1/2}(\Gamma)$, cf. [10]. The energy scalar product is thus given by

$$\langle\!\langle u\,,\,v\rangle\!\rangle := \langle Vu\,,\,v\rangle \quad \text{for all } u, v \in \mathcal{H} = \widetilde{H}^{-1/2}(\Gamma). \tag{44}$$

We consider the lowest-order Galerkin scheme, where $\mathcal{T}_\ell$ is a triangulation of Γ and where $X_\ell := \mathcal{P}^0(\mathcal{T}_\ell)$ denotes the space of all $\mathcal{T}_\ell$-piecewise constant functions on Γ.

As above, we define the local mesh-width function $h_\ell \in \mathcal{P}^0(\mathcal{T}_\ell)$ by $h_\ell|_T := \operatorname{diam}(T)$ for $T \in \mathcal{T}_\ell$.

3.2. Mesh-Refinement. We restrict to the case that the boundary elements $T \in \mathcal{T}_\ell$ are affine line segments for $d = 2$ and planar triangles for $d = 3$, respectively.

In 2D, a marked element $T \in \mathcal{M}_\ell$ is halved into two elements $T_1, T_2 \in \mathcal{T}_{\ell+1}$. To control the K-mesh constant

$$\kappa(\mathcal{T}_\ell) = \max\big\{h_\ell|_T/h_\ell|_{T'} \,:\, T, T' \in \mathcal{T}_\ell \text{ neighbouring elements}\big\}, \tag{45}$$

we recursively do some additional marking: If the neighbour $T' \in \mathcal{T}_\ell$ of a marked element $T \in \mathcal{M}_\ell$ satisfies $h_\ell|_{T'}/h_\ell|_T \geq 2$, we also mark the element T' for refinement. This ensures boundedness $\kappa(\mathcal{T}_\ell) \leq 2\,\kappa(\mathcal{T}_0)$ as $\ell \to \infty$.

In 3D, we use the mesh-refinement introduced in Section 2.2.

3.3. Refinement Indicators. Note that the energy norm $|||\cdot|||$ is nonlocal in the sense that $|||\cdot|||^2 = |||\cdot|||_\Gamma^2$ is not equivalent to $\sum_{T\in\mathcal{T}_\ell} |||\cdot|||_T^2$, where $|||v|||_T^2 = \int_T \int_T u(x)G(x,y)u(y)\,ds_y\,ds_x$, cf. [1]. Therefore, the error estimator η_ℓ does not provide information for a local mesh-refinement directly. Instead, we consider the refinement indicators

$$\mu_\ell(T) = \|h_\ell^{1/2}(\widehat{u}_\ell - u_\ell)\|_{L^2(T)} \quad \text{as well as} \quad \widetilde{\mu}_\ell(T) = \|h_\ell^{1/2}(\widehat{u}_\ell - \Pi_\ell\widehat{u}_\ell)\|_{L^2(T)} \tag{46}$$

for all $T \in \mathcal{T}_\ell$, where Π_ℓ denotes the L^2-projection onto $X_\ell = \mathcal{P}^0(\mathcal{T}_\ell)$. Using a local inverse estimate from [9] and a local approximation result from [3], one can prove estimator equivalence [7]

$$C_1^{-1}\,\eta_\ell \leq \widetilde{\mu}_\ell = \|h_\ell^{1/2}(\widehat{u}_\ell - \Pi_\ell\widehat{u}_\ell)\|_{L^2(\Gamma)} \leq \mu_\ell = \|h_\ell^{1/2}(\widehat{u}_\ell - u_\ell)\|_{L^2(\Gamma)} \leq C_2\,\eta_\ell. \tag{47}$$

The constant C_1 only depends on Γ, whereas C_2 stems from an inverse estimate and additionally depends on the polynomial degree and on the shape regularity constant of the triangulation $\mathcal{T}_\ell$. The proposed mesh-refinement from Section 3.2 thus ensures that C_2 remains uniformly bounded.

Remark. *Note that the definition of h_ℓ has to be consistent with the mesh-refining strategy in the sense that*

$$h_{\ell+1}|_T \leq q\,h_\ell|_T \quad \textit{for all } T \in \mathcal{M}_\ell \tag{48}$$

where $q \in (0,1)$ is a uniform contraction rate. In [4]*, newest vertex bisection, with the slightly non-standard definition $h_\ell|_T = |T|^{1/d}$ instead of $h_\ell|_T = \operatorname{diam}(T)$ is used to ensure* (48)*. In our refinement strategy marked elements are bisec$_5$-refined so that* (48) *holds with the usual definition of h_ℓ and $q = 1/2$.* □

3.4. Convergence of ABEM under the Saturation Assumption. In this section, we prove convergence of ABEM steered by either μ_ℓ or $\widetilde{\mu}_\ell$ from (46). For both error estimators, we prove the estimator reduction (33).

Theorem 7. *Suppose that we use the indicators $\widetilde{\mu}_\ell(T)$ defined in (46) in Algorithm 1. Under the saturation assumption (6), and for any choice of $\theta \in (0,1)$, there are constants $\kappa, \gamma \in (0,1)$ such that the combined error quantity*

$$\widetilde{\Delta}_\ell := |||u - u_\ell|||^2 + |||u - \widehat{u}_\ell|||^2 + \gamma\, \widetilde{\mu}_\ell^2 \tag{49}$$

satisfies the contraction property

$$\widetilde{\Delta}_{\ell+1} \le \kappa \widetilde{\Delta}_\ell. \tag{50}$$

In particular, it holds that $\lim_{\ell\to\infty} |||u - \widehat{u}_\ell||| = \lim_{\ell\to\infty} |||u - u_\ell||| = 0 = \lim_{\ell\to\infty} \widetilde{\mu}_\ell$.

Proof. Recall that $X_\ell \subset X_{\ell+1} \subseteq \widehat{X}_\ell \subset \widehat{X}_{\ell+1}$. Moreover, we note the pointwise estimates $h_\ell/4 \le \widehat{h}_{\ell+1} \le h_\ell/2$ and $h_\ell/16 \le \widehat{h}_{\ell+1} \le h_\ell/4$ for $d = 2, 3$, respectively. Using the fact that the mesh-sizes h_ℓ and $\widehat{h}_{\ell+1}$ are equivalent up to a multiplicative factor, and applying [9, Theorem 4.1], we obtain the inverse estimate

$$\|h_\ell^{1/2} \widehat{v}_{\ell+1}\|_{L^2(\Gamma)} \le C_{\rm inv}\, |||\widehat{v}_{\ell+1}||| \quad \text{for all } \widehat{v}_{\ell+1} \in \widehat{X}_{\ell+1}. \tag{51}$$

In 2D, the constant $C_{\rm inv} > 0$ only depends on the mesh-ratio $\kappa(\widehat{\mathcal{T}}_{\ell+1}) \le 2\kappa(\mathcal{T}_0)$. In 3D, the constant $C_{\rm inv} > 0$ only depends on the smallest interior angle in $\widehat{\mathcal{T}}_{\ell+1}$, and in particular, since $\widehat{\mathcal{T}}_{\ell+1}$ is obtained from $\mathcal{T}_0$ by certain newest vertex bisections, it depends only on the smallest interior angle in $\mathcal{T}_0$.

We use the triangle inequality, the $\mathcal{T}_{\ell+1}$-piecewise orthogonality of $\Pi_{\ell+1}$, and the inverse estimate (51) to obtain

$$\begin{aligned}
\widetilde{\mu}_{\ell+1} &= \|h_{\ell+1}^{1/2}(1 - \Pi_{\ell+1})\widehat{u}_{\ell+1}\|_{L^2(\Gamma)} \\
&\le \|h_{\ell+1}^{1/2}(1 - \Pi_{\ell+1})\widehat{u}_\ell\|_{L^2(\Gamma)} + \|h_{\ell+1}^{1/2}(1 - \Pi_{\ell+1})(\widehat{u}_{\ell+1} - \widehat{u}_\ell)\|_{L^2(\Gamma)} \\
&\le \|h_{\ell+1}^{1/2}(1 - \Pi_{\ell+1})\widehat{u}_\ell\|_{L^2(\Gamma)} + \|h_{\ell+1}^{1/2}(\widehat{u}_{\ell+1} - \widehat{u}_\ell)\|_{L^2(\Gamma)} \\
&\le \|h_{\ell+1}^{1/2}(1 - \Pi_{\ell+1})\widehat{u}_\ell\|_{L^2(\Gamma)} + C_{\rm inv}\, |||\widehat{u}_{\ell+1} - \widehat{u}_\ell|||.
\end{aligned}$$

To estimate the second term, we now proceed precisely as in the proof of Theorem 4 (AFEM) to verify that

$$\|h_{\ell+1}^{1/2}(\widehat{u}_\ell - \Pi_{\ell+1}\widehat{u}_\ell)\|_{L^2(\Gamma)}^2 \le \varrho\, \widetilde{\mu}_\ell^2,$$

where $\varrho = 1 - \theta$. Using the same notation as in the proof of Theorem 4, we obtain the estimator reduction (33) with $C_\delta = (1 + \delta^{-1}) C_{\rm inv}^2$. □

Theorem 8. *Suppose that we use the indicators $\mu_\ell(T)$ defined in (46) in Algorithm 1. Under the saturation assumption (6), and for any choice of $\theta \in (0,1)$, there are constants $\kappa, \gamma \in (0,1)$ such that*

$$\Delta_\ell := |||u - u_\ell|||^2 + |||u - \widehat{u}_\ell|||^2 + \gamma\, \mu_\ell^2 \tag{52}$$

satisfies the contraction property

$$\Delta_{\ell+1} \le \kappa \Delta_\ell. \tag{53}$$

In particular, Algorithm 1 is convergent, that is, $\lim_{\ell\to\infty} |||u-\widehat{u}||| = \lim_{\ell\to\infty} |||u-u_\ell||| = 0 = \lim_{\ell\to\infty} \mu_\ell$.

Proof. The triangle inequality and the inverse estimate (51) prove

$$\begin{aligned}\mu_{\ell+1} &= \|h_{\ell+1}^{1/2}(\widehat{u}_{\ell+1}-u_{\ell+1})\|_{L^2(\Gamma)}\\ &\le \|h_{\ell+1}^{1/2}(\widehat{u}_\ell-u_\ell)\|_{L^2(\Gamma)} + \|h_{\ell+1}^{1/2}((\widehat{u}_{\ell+1}-u_{\ell+1})-(\widehat{u}_\ell-u_\ell))\|_{L^2(\Gamma)}\\ &\le \|h_{\ell+1}^{1/2}(\widehat{u}_\ell-u_\ell)\|_{L^2(\Gamma)} + C_{\rm inv}\,|||(\widehat{u}_{\ell+1}-\widehat{u}_\ell)-(u_{\ell+1}-u_\ell)|||.\end{aligned}$$

The mesh-refinement rule from Section 3.2 yields the properties

$$\begin{aligned} h_{\ell+1}|_T &\le \frac{1}{2}\,h_\ell|_T \quad \text{for all } T\in\mathcal{M}_\ell,\\ \text{and}\quad h_{\ell+1}|_T &\le h_\ell|_T \quad \text{for all } T\in\mathcal{T}_\ell\backslash\mathcal{M}_\ell.\end{aligned}$$

Dörfler's marking strategy (8) gives

$$\begin{aligned}\|h_{\ell+1}^{1/2}(\widehat{u}_\ell-u_\ell)\|_{L^2(\Gamma)}^2 &= \sum_{T\in\mathcal{M}_\ell}\|h_{\ell+1}^{1/2}(\widehat{u}_\ell-u_\ell)\|_{L^2(T)}^2 + \sum_{T\in\mathcal{T}_\ell\backslash\mathcal{M}_\ell}\|h_{\ell+1}^{1/2}(\widehat{u}_\ell-u_\ell)\|_{L^2(T)}^2\\ &\le \frac{1}{2}\sum_{T\in\mathcal{M}_\ell}\|h_\ell^{1/2}(\widehat{u}_\ell-u_\ell)\|_{L^2(T)}^2 + \sum_{T\in\mathcal{T}_\ell\backslash\mathcal{M}_\ell}\|h_\ell^{1/2}(\widehat{u}_\ell-u_\ell)\|_{L^2(T)}^2\\ &= -\frac{1}{2}\sum_{T\in\mathcal{M}_\ell}\mu_\ell(T)^2 + \sum_{T\in\mathcal{T}_\ell}\mu_\ell(T)^2\\ &\le \Big(1-\frac{\theta}{2}\Big)\sum_{T\in\mathcal{T}_\ell}\mu_\ell(T)^2\\ &= \varrho\,\mu_\ell^2,\end{aligned}$$

with $\varrho := \big(1-\theta/2\big) < 1$. For any $\delta>0$, Young's inequality then proves

$$\begin{aligned}\mu_{\ell+1}^2 &\le (1+\delta)\varrho\,\mu_\ell^2 + (1+\delta^{-1})C_{\rm inv}^2\,|||(\widehat{u}_{\ell+1}-\widehat{u}_\ell)-(u_{\ell+1}-u_\ell)|||^2\\ &= (1+\delta)\varrho\,\mu_\ell^2 + (1+\delta^{-1})C_{\rm inv}^2\big(|||\widehat{u}_{\ell+1}-\widehat{u}_\ell|||^2 + |||u_{\ell+1}-u_\ell|||^2\big),\end{aligned}$$

where we have used Galerkin orthogonality and $X_\ell\subset X_{\ell+1}\subseteq\widehat{X}_\ell\subset\widehat{X}_{\ell+1}$. Using the same notation as in the proof of Theorem 4, we now have proven the estimator reduction (33) with $C_\delta = (1+\delta^{-1})C_{\rm inv}^2$. □

4. Numerical Experiments

In the following section, we present three numerical experiments to underline our theoretical findings. Throughout, the energy error is computed by the Galerkin orthogonality

$$|||u-u_\ell|||^2 = |||u|||^2 - |||u_\ell|||^2. \tag{54}$$

Note that discrete energies $|||u_\ell|||^2$ can be computed by use of the Galerkin matrix. The exact energy $|||u|||^2$ is extrapolated by Aitken's Δ^2-method applied to certain discrete energies $|||u_\ell|||^2$

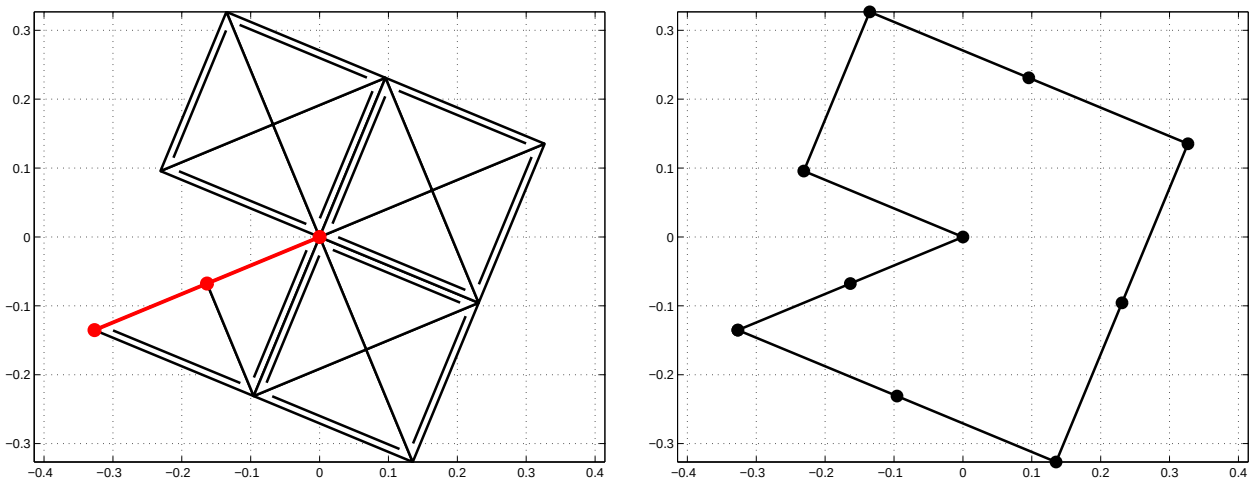

FIGURE 4. Initial mesh in FE Example 4.1 with 14 rectangular elements (left) and initial mesh in BE Example 4.2 with 10 affine boundary segments (right). The reference edges for the newest vertex bisection in the FE mesh are indicated by double lines, and the nodes on the Dirichlet boundary are indicated by red bullets (left).

corresponding to a sequence of uniformly refined meshes. Here, uniform refinement means that, for 2D FEM or 3D BEM, all triangles are split into 4 similar son triangles ba halving its edges, whereas boundary segments in 2D BEM are split into 2 son segments of half length.

Besides the Galerkin error $|||u - u_\ell|||$, we plot the natural h-$h/2$-error estimators η_ℓ as well as the (problem dependent) error estimator $\widetilde{\mu}_\ell$. We empirically compare uniform mesh-refinement with $\widetilde{\mu}_\ell$-steered mesh-refinement. Throughout, Algorithm 1 turns out to be effective in the sense that even the optimal rate of convergence is recovered.

4.1. Finite Element Method. In the first experiment, we consider the numerical solution of (10). The domain $\Omega \subset \mathbb{R}^2$, visualized in Figure 4, is a rotated Z-shape which is obtained by rotation of $(-0.25, 0.25)^2 \backslash \mathrm{conv}\{(0,0), (-0.25, -.025), (0, -0, 25)\}$ with angle $-\pi/8$. The exact solution reads

$$u(x) = r^{4/7} \cos(4\varphi/7) \quad \text{in polar coordinates } x = r\,(\cos\varphi, \sin\varphi) \tag{55}$$

and has a generic singularity at the re-entrant corner $(0,0)$. We stress that the rotation of the Z-shape is done in a way that provides homogeneous Dirichlet data at the two diagonal boundary edges, cf. Figure 4. The initial mesh $\mathcal{T}_0$ consisted of $N = 14$ rectangular triangles, where the longest edges are the reference edges.

Recall that, for a piecewise H^2 solution, the optimal order of convergence in this experiment is $\mathcal{O}(N^{-1/2})$, where $N = \#\mathcal{T}$ is the number of elements. Figure 5 provides the experimental results for uniform and adaptive mesh-refinement, where we use

$$\widetilde{\zeta}_\ell = (\widetilde{\mu}_\ell^2 + \mathrm{osc}_\ell^2)^{1/2}$$

and $\theta = 0.25$ for marking in the adaptive algorithm. Adaptive mesh-refinement is performed as described in Section 2.2. We stress that Theorem 4 predicts convergence of this adaptive

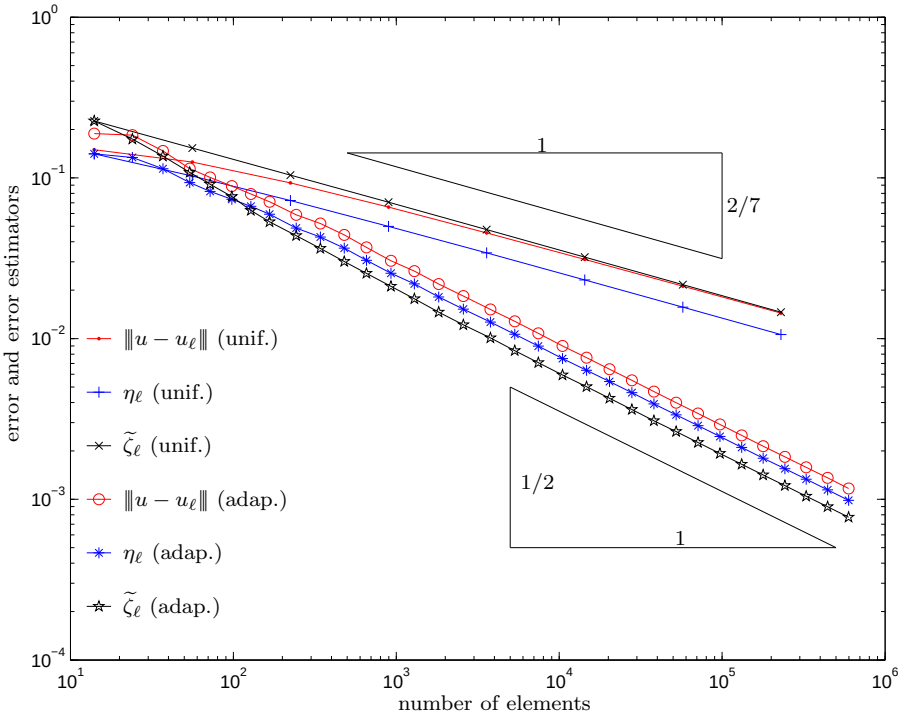

FIGURE 5. Error $|||u - u_h||| = \|\nabla(u - u_h)\|_{L^2(\Omega)}$ and error estimators η_ℓ and $\widetilde{\zeta}_\ell = (\widetilde{\mu}_\ell^2 + \mathrm{osc}_\ell^2)^{1/2}$ for uniform and adaptive FEM in Example 4.1, where we use $\theta = 0.25$ and $\widetilde{\zeta}_\ell$ for marking in Algorithm 1. Note that the adaptive strategy yields the optimal order of convergence.

scheme. Uniform mesh-refinement leads to a suboptimal order of convergence $\mathcal{O}(N^{-2/7})$. The optimal order of convergence $\mathcal{O}(N^{-1/2})$ is recovered by use of the adaptive algorithm.

4.2. Boundary Element Method in 2D. In this experiment, we consider Symm's integral equation

$$Vu = (K + 1/2)g \tag{56}$$

which is equivalent to the Dirichlet problem

$$\begin{aligned} -\Delta U &= 0 \quad \text{in } \Omega, \\ U &= g \quad \text{on } \Gamma. \end{aligned} \tag{57}$$

In this case, the exact solution of (56) is the normal derivative $u = \partial_n U$ of $U \in H^1(\Omega)$, and U can obtained from (u, g) by use of Green's third formula [10]. Kg denotes the double-layer potential, which is formally defined defined as the Cauchy principal value

$$(Kg)(x) = \int\!\!\!\!\!\!-_\Gamma \partial_{n(y)} G(s, y)\, g(y)\, ds_y \quad \text{for } x \in \Gamma$$

and then extended to a linear operator on $H^{1/2}(\Gamma)$ by continuity. We consider the rotated Z-shape Ω of Experiment 4.1, and the exact solution of (57) is given by (55). We stress

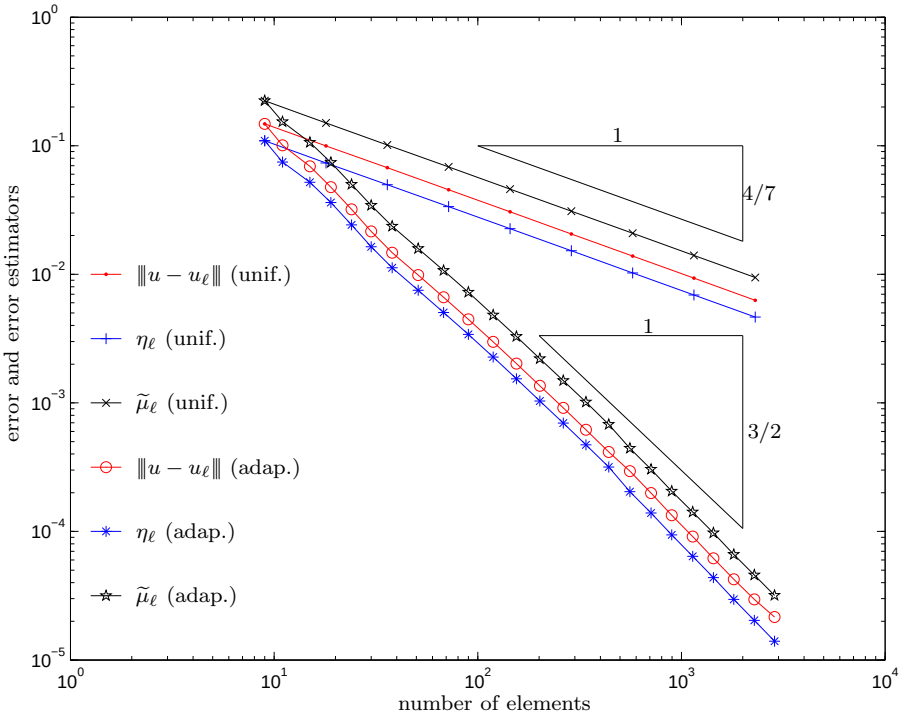

FIGURE 6. Error $|||u-u_\ell||| \sim \|u-u_\ell\|_{H^{-1/2}(\Gamma)}$ and error estimators η_ℓ and $\widetilde{\mu}_\ell$ for uniform and adaptive BEM in Example 4.2, where we use $\theta = 0.25$ and $\widetilde{\mu}_\ell$ for marking in Algorithm 1. Note that the adaptive strategy yields the optimal order of convergence.

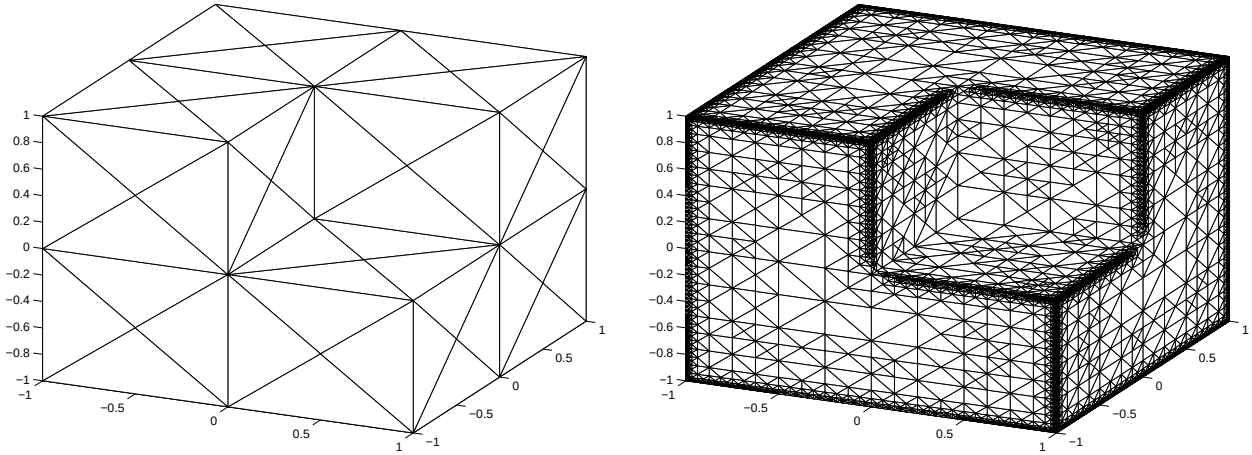

FIGURE 7. Initial mesh with $N = 96$ rectangular triangles (left) and $\widetilde{\mu}_\ell$-adaptively generated mesh with $N = 20.806$ triangles (right) in Example 4.3.

that Ω is scaled in a way that guarantees $\operatorname{diam}(\Omega) < 1$ to ensure ellipticity of the single-layer potential. The initial BE mesh $\mathcal{T}_0$ with $N = 10$ affine boundary segments is shown in Figure 4.

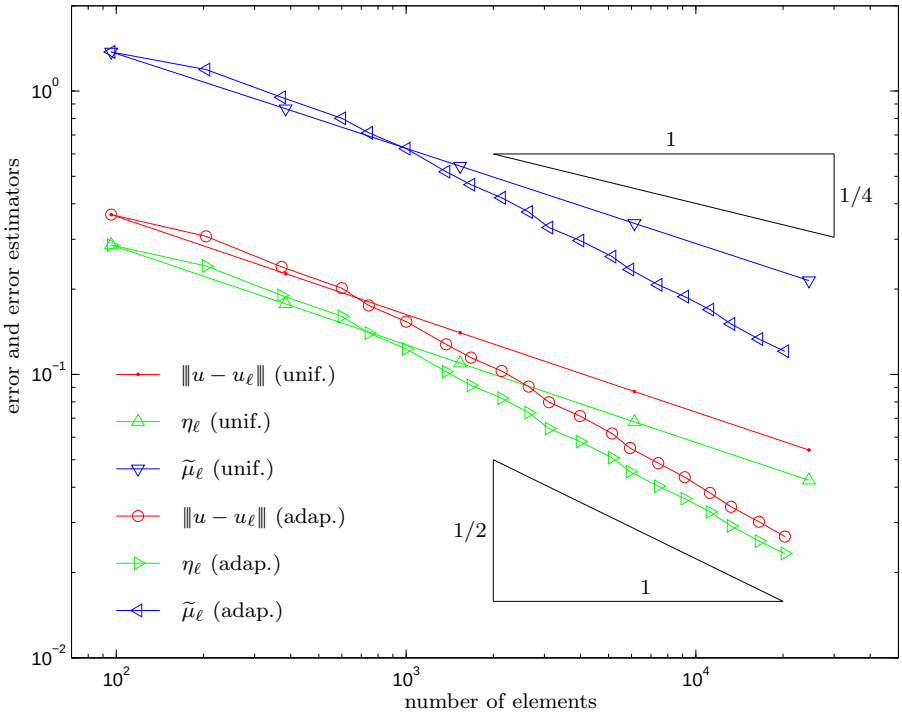

FIGURE 8. Error $|\!|\!|u-u_\ell|\!|\!| \sim \|u-u_\ell\|_{H^{-1/2}(\Gamma)}$ and error estimators η_ℓ and $\widetilde{\mu}_\ell$ for uniform and isotropic adaptive BEM in Example 4.3, where we use $\theta = 0.25$ and $\widetilde{\mu}_\ell$ for marking in Algorithm 1.

If the normal derivative $u = \partial U/\partial n$ of U is a piecewise H^1 function then the optimal order of convergence in this experiment is $\mathcal{O}(N^{-3/2})$, in terms of the number $N = \#\mathcal{T}$ of elements [12]. The numerical results are shown in Figure 6, where we again use $\theta = 0.25$ and $\widetilde{\mu}_\ell$ for marking in the adaptive algorithm. The adaptive mesh-refinement is performed as described in Section 3.2. Uniform mesh-refinement leads to a suboptimal order of convergence $\mathcal{O}(N^{-4/7})$. This is cured by the adaptive algorithm in the sense that the optimal order of convergence is recovered.

For both, uniform and adaptive mesh-refinement, we observe that the error estimators η_ℓ and μ_ℓ remain parallel with $|\!|\!|u-u_\ell|\!|\!|$. This strongly indicates reliability of η_ℓ and thus numerically verifies the saturation assumption (6) for this experiment.

4.3. Boundary Element Method in 3D. Finally, we compute the discrete solution of Symm's integral equation

$$Vu = 1 \quad \text{on } \Gamma$$

with Γ the boundary of the Fichera cube $\Omega = [-1,1]^3 \setminus ([0,1] \times [-1,0] \times [0,1])$. Figure 7 shows the uniform initial mesh $\mathcal{T}_0$ consisting of $N = 96$ rectangular triangles.

To illustrate the performance of Algorithm 1, Figure 8 shows the error $|\!|\!|u-u_\ell|\!|\!|$ and the estimators η_ℓ and $\widetilde{\mu}_\ell$ for uniform and adaptive mesh-refinements. For adaptive mesh-refinement, we use $\theta = 0.25$ and $\widetilde{\mu}_\ell$ in Algorithm 1. Moreover, we use the bisec$_5$-based mesh-refinement from Section 2.2. We observe that uniform mesh-refinement leads to a suboptimal order of convergence of approximately $\mathcal{O}(N^{-1/4})$. The isotropic adaptive strategy leads to

an improved order of approximately $\mathcal{O}(N^{-1/2})$. This, as expected, is not optimal since isotropic mesh-refinement does not resolve the generic edge-singularities efficiently [7]. For this fact, the reader is also refered to some heuristics from [2]. As in the previous example, both adaptive and uniform mesh-refinement suggest reliability of η_ℓ. This gives empirical evidence for the saturation assumption (6), which is required in Theorem 7 to guarantee convergence of the adaptive scheme.

Acknowledgement. Parts of the results have been achieved during a research stay of C.O. and D.P. at the Hausdorff Institute for Mathematics in Bonn, which is thankfully acknowledged. S.F. acknowledges a grant of the graduate school *Differential Equations – Models in Science and Engineering*, funded by the Austrian Science Fund (FWF) under grant W800-N05.

References

[1] C. Carstensen, B. Faermann, *Mathematical foundation of a posteriori error estimates and adaptive mesh-refining algorithms for boundary integral equations of the first kind*, Eng. Anal. Bound. Elem. **25** (2001), 497–509.

[2] C. Carstensen, M. Maischak, D. Praetorius, E. P. Stephan, *Residual-based a posteriori error estimate for hypersingular equation on surfaces.* Numer. Math. **97** (2004), no. 3, 397–425.

[3] C. Carstensen, D. Praetorius, *Averaging techniques for the effective numerical solution of Symm's integral equation of the first kind*, SIAM J. Sci. Comput. **27** (2006), 1226–1260.

[4] J. Cascon, C. Kreuzer, R. Nochetto, K. Siebert, *Quasi-optimal convergence rate for an adaptive finite element method*, SIAM J. Numer. Anal. **46** (2008), 2524–2550.

[5] W. Dörfler, *A convergent adaptive algorithm for Poisson's equation*, SIAM J. Numer. Anal. **33** (1996), 1106–1124.

[6] W. Dörfler, R. Nochetto, *Small data oscillation implies the saturation assumption*, Numer. Math. **91** (2002), 1–12.

[7] S. Ferraz-Leite, D. Praetorius, *Simple a posteriori error estimators for the h-version of the boundary element method*, Computing **83** (2008), 135–162.

[8] S. Funken, D. Praetorius, P. Wissgott, *Efficient implementation of adaptive P1-FEM in MATLAB*, ASC Report **19/2008**, Institute for Analysis and Scientific Computing, Vienna University of Technology 2008.

[9] I. Graham, W. Hackbusch, S. Sauter, *Finite elements on degenerate meshes: Inverse-type inequalities and applications*, IMA J. Numer. Anal. **25** (2005), 379–407.

[10] W. McLean, *Strongly elliptic systems and boundary integral equations*, Cambridge University Press, Cambridge, 2000.

[11] P. Morin, R. Nochetto, K. Siebert, *Data oscillation and convergence of adaptive FEM*, SIAM J. Numer. Anal. **38** (2000), 466–488.

[12] S. Sauter, C. Schwab, *Randelementmethoden: Analyse, Numerik und Implementierung schneller Algorithmen*, Teubner Verlag, Wiesbaden, 2004.

[13] R. Verfürth, *A posteriori error estimation and adaptive mesh refinement techniques*, J. Comput. Appl. Math. **50** (1994), 67–83.

[14] R. Verfürth, *A review of a posteriori error estimation and adaptive mesh-refinement techniques*, Teubner, Stuttgart, 1996.

Institute for Analysis and Scientific Computing, Vienna University of Technology, Wiedner Hauptstrasse 8-10, A-1040 Wien, Austria

E-mail address: {Samuel.Ferraz-Leite,Dirk.Praetorius}@tuwien.ac.at

Oxford University, Computing Laboratory, Wolfson Building, Parks Road, Oxford OX1 3QD, UK
E-mail address: Christoph.Ortner@comlab.ox.ac.uk